IOP Conf. Series: Materials Science and Engineering **227** (2017) 012088 doi:10.1088/1757-899X/227/1/012088

Numerical investigation of shallow water effect on a barge ship resistance

F Pacuraru[1] **and L Domnisoru**[2]
[1,2] Department of Naval Architecture
"Dunarea de Jos" University of Galati, Domneasca Street 111, 800201, Romania

E-mail: leonard.domnisoru@ugal.ro

Abstract. The inland waterway cargo transport has extended over the decades, bringing up specific technical issues. From the hydrodynamics point of view, for the inland ships one of the most challenging issue is the effect of shallow water on the ship resistance. In the present study, there are developed numerical analyses for the viscous flow around a barge hull in the case of the shallow water fluid domain. The barge hull has prismatic shapes, in the cargo holds areas, with vertical sides, and geometric non-linear shapes more significant at the fore part. The hull shape CAD model is developed by Rhinoceros software. The numerical analyses are performed by CFD RANS-VOF method, with free surface and shallow-water, using the NUMECA / FineMarine software, having free sinkage and trim conditions. The shallow-water flow induces significant hydrodynamic non-linearities in compare to the deep-water flows. Several ship speeds and water depths are considered. We have focused on the identification of the ship's induced waves system and the resulting barge resistance. The conclusions of this study are stressing out the significant influence of the shallow-water conditions on the barge resistance, making possible to draw up practical technical information's for the barge hull design.

Keywords: barge, shallow water, ship resistance, RANS –VOF techniques, CFD method.

1. Introduction

The inland waterway cargo transport has an important role all over the world. This solution can compete with the highway and railway cargo transports, with reduced pollution effects, as low energy consumption, noise and noxious. The inland navigation is requiring the ships' operation under restricted fairway conditions [1]. The inland ship's dimensions have to comply with the existing waterway infrastructure, reduced length, breadth and draught, according to the locks and bridges capabilities. Also the hull and cargo holds structures must comply with the national and international rules for safety inland navigation.

The prediction of an inland ship hydrodynamic resistance in shallow water conditions is important for the estimation of the onboard power design requirements. Shallow water can affect viscous and wave resistance, sinkage and trim, propulsive efficiency, and far-field wave systems [2]. Van der Meij [3] used the non-linear panel method and the RANS methods for the improvement of a bow and stern shape of an inland ship, considering the influence of the limited depth. Rankine source method has been used also by Lungu and Pacuraru [4] in order to evaluate the effects of shallow water on a tanker barge. Raven [2] has used CFD RANS techniques in order study effect of depth variation on viscous resistance on scale effects. Rotteveel and Hekkenberg [5] have studied hull form variation and shallow water influence in order to improve the inland ship design guidelines. Ship squat prediction on KRISO container ship was studied by Jachowski [6], using RANS-VOF method, and for a inland barge by

Tabaczek [7], both using Fluent code. Tezdogan, Incecik and Turan [8] have used Star-CCM code to predict heave and pitch motions, at full-scale, in shallow water conditions.

We are focused on a computational study based on the free-surface capturing RANS-VOF approach. NUMECA/FineMarine commercial code has been used to evaluate the flow field around barge navigating in shallow water. The solver computes the incompressible RANS equations on unstructured Cartesian mesh using finite volume method formulation, involving k-ω SST turbulence model. As long as the hull shape investigated in the present work is a non-self-propelled barge, our analysis focuses on the influence of the variation of water depth on barge own wave and viscous resistance, but also on solving the free sinkage and trim barge condition. The main dimensions of the barge are presented in table 1 and the main characteristics in figure 1.

Table 1. The main dimensions of the Europe 2B barge hull.

Dimension	***Symbol***	***Value [m]***
Length overall	*L*	76.50
Breadth	*B*	10.96
Depth	*D*	3.20
Draught	*T*	2.70

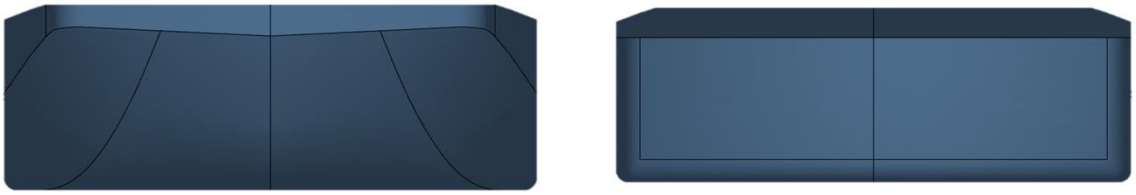

Figure 1. The Europe 2B barge hull. Bow view (left) and stern view (right).

2. Computational strategy

The NUMECA/FineMarine code has been used to compute the flow solution on a multi-block, in parallel computing approach. The RANS solver is fully implicit, based on the finite volume method to build up the 3D discretization of the transport equations. The velocity and pressure are obtained from the momentum and continuity equations. In the case of turbulent flows, additional transport equations for modelled variables are discretized and solved using the same principles according to Duvigneau, Visonneau, Deng and Queutey [9,10]. The k-ω SST turbulence model with wall function formulation is used for turbulence closure in this study. Free-surface capturing strategy is based on multi-phase flow approach using Volume of Fluid method with high-resolution interface schemes. Incompressible and non-miscible flow phases are modelled through the use of conservation equations for each volume fraction of phase / fluid, according to Queutey and Visonneau [11]. The velocity-pressure coupling is handled by SIMPLE approach, based on pressure equation formulation. Six degrees of freedom can be modelled by the software. Several degrees of freedom can be restrained in simulation.

Seven Cartesian mono-block unstructured grids between 2.3 and 2.8 million cells have been generated to cover the entire computational domain along the barge hull, for each depth case considered. The domain covers one ship length upstream of the bow, half above, one and a half ship length out from the side and bottom of the hull, and two ship lengths downstream of the stern. A grid refinement has been performed on the bow and the stern part of the hull as one can see in figure 2. Layers of high aspect ratio cells tangentially to the ship hull and bottom wall have been inserted in the Eulerian mesh, in order to capture viscous effects. An analytical weighting mesh deformation approach is employed as long as both trim and sinkage were solved during the computations.

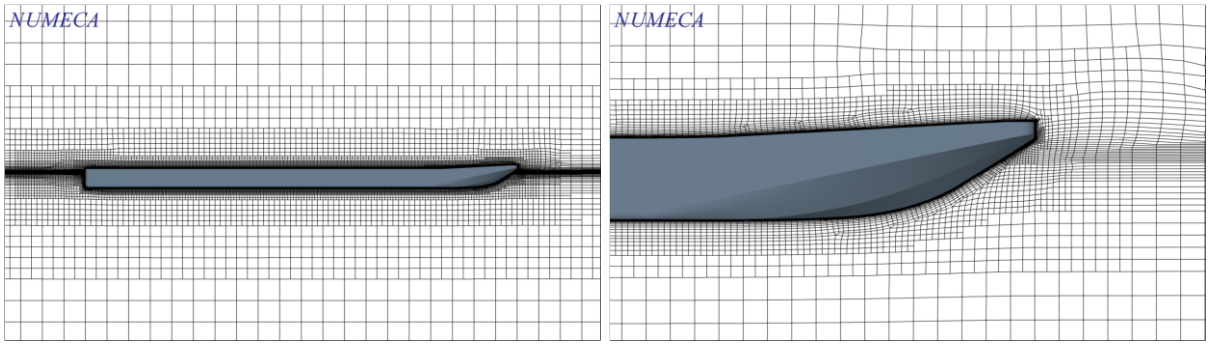

Figure 2. Cartesian mesh generated around the barge hull.

To improve computation efficiency, for cases that involves many speeds, the calculation has been initialized from the previous (lower) speed that already has been converged. Using this strategy, acceleration time is significantly reduced and also the time for ship to reach the equilibrium position.

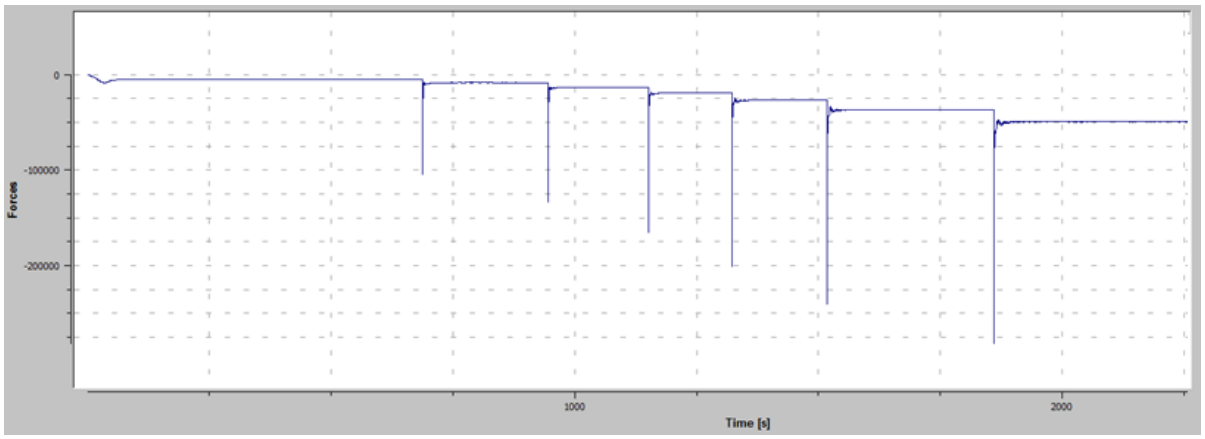

Figure 3. Convergence history.

3. Computational results

The present study considers a systematically full scale ship resistance calculation in calm water for an inland barge which navigates at six different water depths situation. Unrestricted water calculations were also performed as a reference case for comparisons. For most inland ships, which navigate at moderate and low speeds, the shallow water effect becomes important when water depth-to-ship draft ratios (H/T) are less than 4.0. Since most inland ships operate in channels at small H/T, typically less than 1.5, shallow-water effects have major impacts on ship navigation. For the present work, six water depths corresponding to H/T from 1.5 to 4 were considered. The ship resistance was computed for seven speeds (v) ranging from 6 to 18 km/h and for a draught of 2.70 m. Table 2 gives the total resistance computed for all cases (combinations v and H/T) studied during the present research. The solutions computed in table 2 are plotted in figure 4.

The results show an increasing of total ship resistance when the H/T ratio decreases and it becomes more significant for higher speeds, as expected. That appears due to pressure drag resistance increase. Table 3, which includes the relative increasing of total resistance, reveals an unexpected increasing of total resistance of 73% and 110%, for H/T=1.5 and speeds of v=16; 18 km/h, respectively. Deeper investigation of the flow characteristics shows that green water phenomena appear for those speeds as one can see in figure 5 and figure 6, which explains the reason for the major instantaneous increasing of the barge resistance. Another argument that sustains this statement is the trim trend change (table 4) and a significant increased sinkage (table 5) at H/T=1.5.

Table 2. Total resistance computed in this study.

	H/T		**1.5**	**2.0**	**2.5**	**3.0**	**3.5**	**4.0**	***unrestricted***
No.	***v*[m/s]**	***v*[km/h]**	***Rt*[kN]**	***Rt*[kN]**	***Rt*[kN]**	***Rt*[kN]**	***Rt*[kN]**	***Rt*[kN]**	***Rt*[kN]**
1	1.67	6	13.07	11.59	11.11	10.41	10.42	10.27	9.74
2	2.23	8	22.95	20.77	19.37	18.28	18.31	17.90	16.88
3	2.79	10	36.98	32.67	30.52	28.87	28.71	27.94	26.41
4	3.35	12	55.82	48.18	44.82	42.42	42.12	40.70	38.82
5	3.91	14	80.00	68.43	62.85	59.89	60.00	58.24	53.88
6	4.47	16	126.58	96.62	89.86	82.97	81.73	78.85	73.88
7	5.03	18	208.10	132.66	125.07	114.70	112.27	106.85	98.72

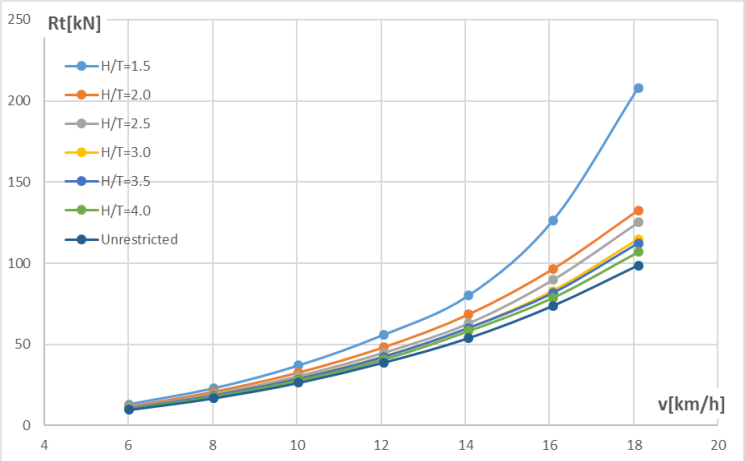

Figure 4. Total ship resistance curves comparison.

Table 3. Shallow water effect on ship resistance (with reference to the unrestricted depth).

No.	**v[km/h] : H/T**	**1.5**	**2.0**	**2.5**	**3.0**	**3.5**	**4.0**
1	6	34.26%	19.04%	14.14%	6.98%	7.04%	5.50%
2	8	35.97%	23.08%	14.75%	8.34%	8.49%	6.05%
3	10	40.05%	23.72%	15.59%	9.34%	8.71%	5.81%
4	12	43.80%	24.13%	15.47%	9.30%	8.51%	4.85%
5	14	48.48%	27.01%	16.65%	11.16%	11.36%	8.09%
6	16	71.33%	30.77%	21.63%	12.30%	10.62%	6.72%
7	18	110.80%	34.38%	26.69%	16.19%	13.73%	8.24%

The wave profiles plotted in figure 7 for speed 12 km/h reveal a slightly change of the barge own wave phase and as well the increase of the wave height. Due to the sinkage (table 4), the eigen wave median plane is shifted in vertical direction, having the calm water plane reference, so that there can be noticed in the figure 7 the differences between the wave profiles.

Due to the hydrodynamic interaction between the hull bottom and the waterway floor several changes are recorded. The flow velocity in the domain between the hull bottom and the waterway floor has higher values and leads to a significant change of the dynamic pressure and an increase of the sinkage, trim and resistance. The variation of the pressure distribution on the waterway floor is presented in figure 8 and figure 10. In order to identify the system of waves changes corresponding to different depth, a set of pictures present the wave pattern in figure 9 and figure 11.

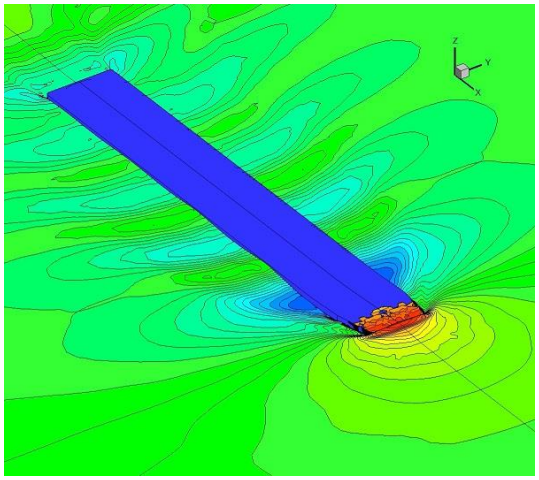

Figure 5. Green water at v=16km/h.

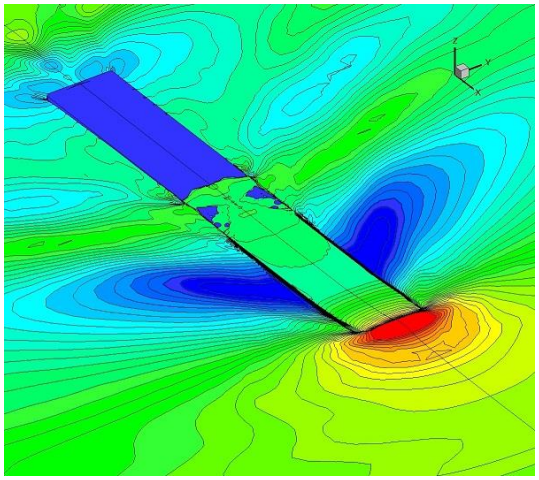

Figure 6. Green water at v=18km/h.

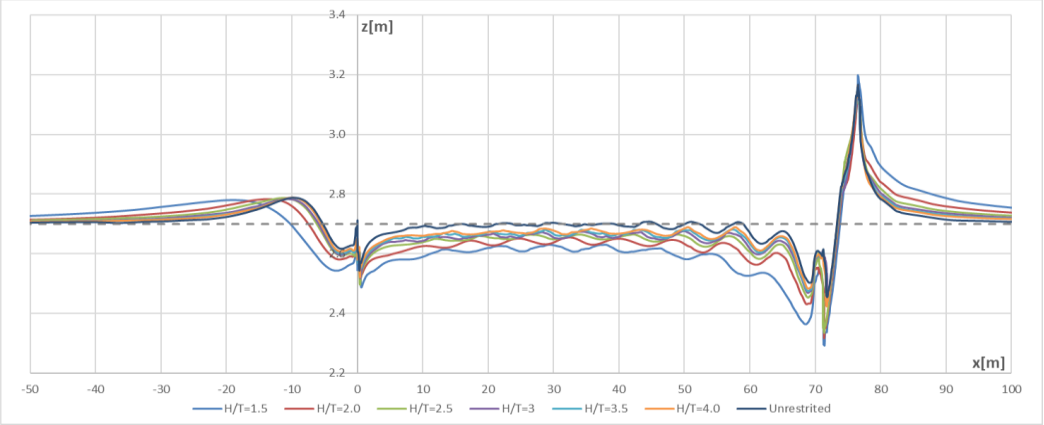

Figure 7. Comparison of wave profiles computed for v=12 km/h at the six depths.

Table 4. Variation of barge sinkage.

No.	***v*[km/h] : *H/T***	**1.5**	**2.0**	**2.5**	**3.0**	**3.5**	**4.0**
1	6	-0.025	-0.020	-0.015	-0.012	-0.011	-0.009
2	8	-0.049	-0.035	-0.029	-0.024	-0.021	-0.019
3	10	-0.082	-0.059	-0.047	-0.039	-0.034	-0.030
4	12	-0.130	-0.090	-0.071	-0.059	-0.051	-0.046
5	14	-0.199	-0.132	-0.102	-0.084	-0.073	-0.065
6	16	-0.318	-0.189	-0.143	-0.114	-0.098	-0.087
7	18	-0.407	-0.276	-0.198	-0.155	-0.131	-0.116

Table 5. Variation of barge trim.

No.	***v*[km/h] : *H/T***	**1.5**	**2.0**	**2.5**	**3.0**	**3.5**	**4.0**
1	6	0.001	-0.002	-0.002	-0.001	-0.001	-0.001
2	8	0.003	-0.003	-0.004	-0.003	-0.003	-0.002
3	10	0.004	-0.006	-0.008	-0.005	-0.004	-0.004
4	12	0.008	-0.009	-0.013	-0.008	-0.007	-0.006
5	14	0.023	-0.012	-0.019	-0.013	-0.012	-0.011
6	16	0.093	-0.015	-0.030	-0.020	-0.019	-0.017
7	18	0.136	-0.003	-0.049	-0.029	-0.030	-0.028

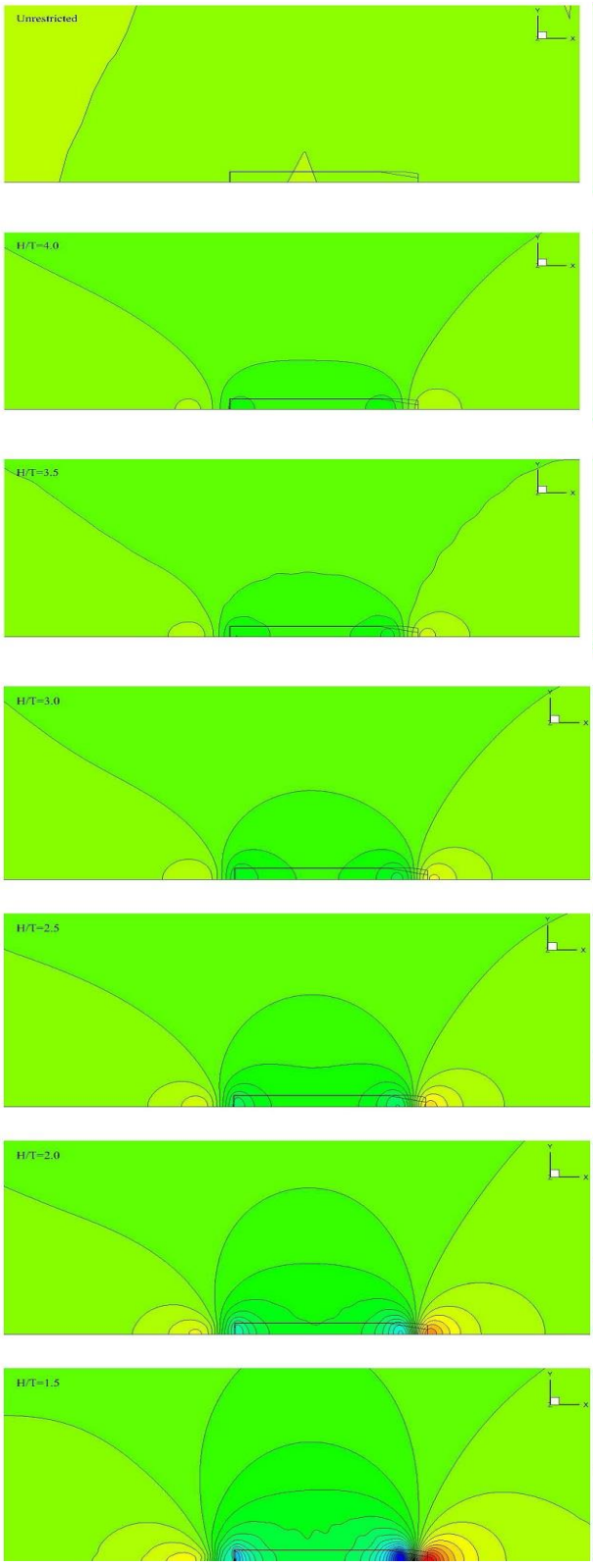

Figure 8. Pressure distribution on the waterway floor at v=12km/h, function to water depth (H/T=1.5 – 4.0).

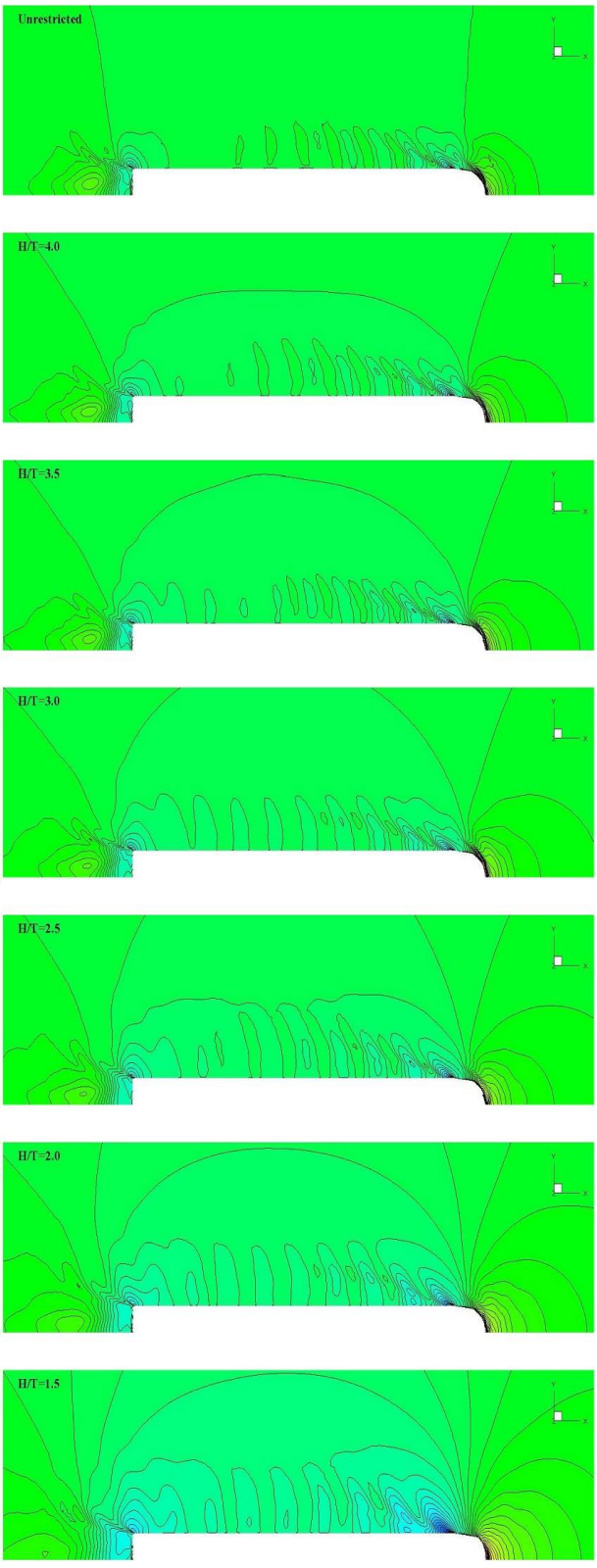

Figure 9. Wave patterns at v=12km/h, function to water depth (H/T=1.5 – 4.0).

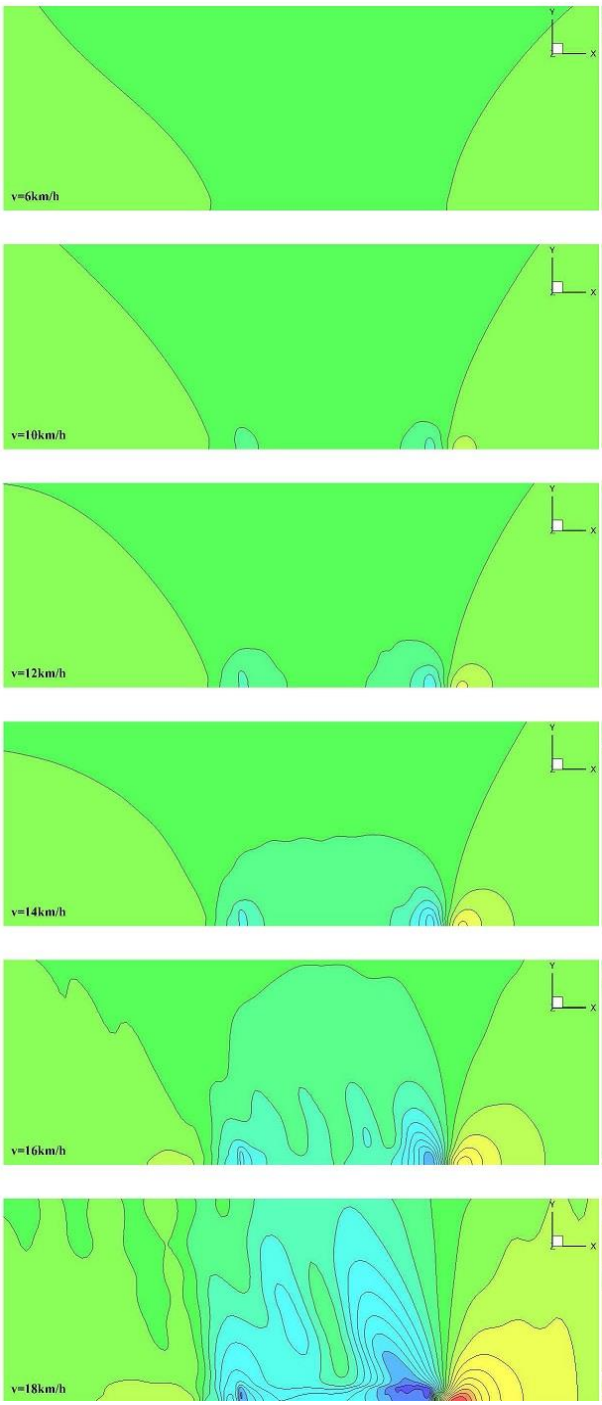

Figure 10. Pressure distribution on the waterway floor for H/T=1.5, function to the ship speed (v=6-18 km/h).

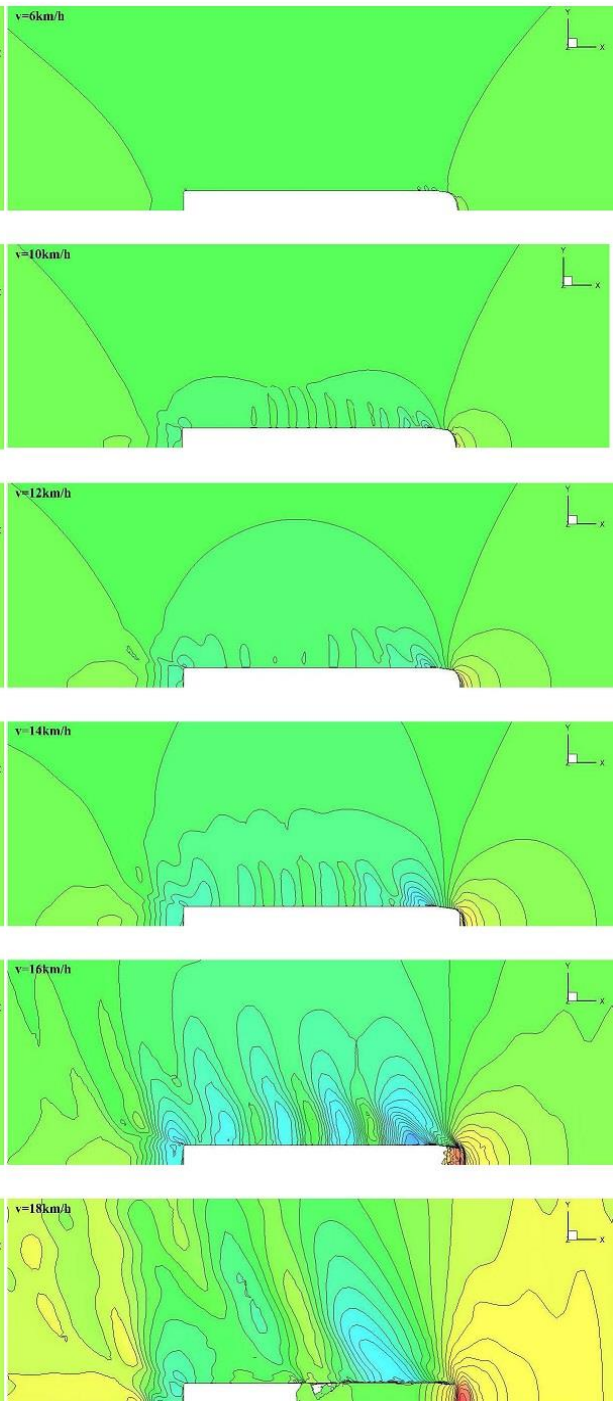

Figure 11. Wave patterns on H/T=1.5, function to the ship speed (v=6-18 km/h).

Due to the shallow-water condition, around the body the water velocity increases, according to Bernoulli law, and induces a modification of the pressure distribution under the ship hull, as it can be seen in figure 12 and also on the waterway floor. Moreover, the accelerated water can pull the vessel down determining the sink of the ship.

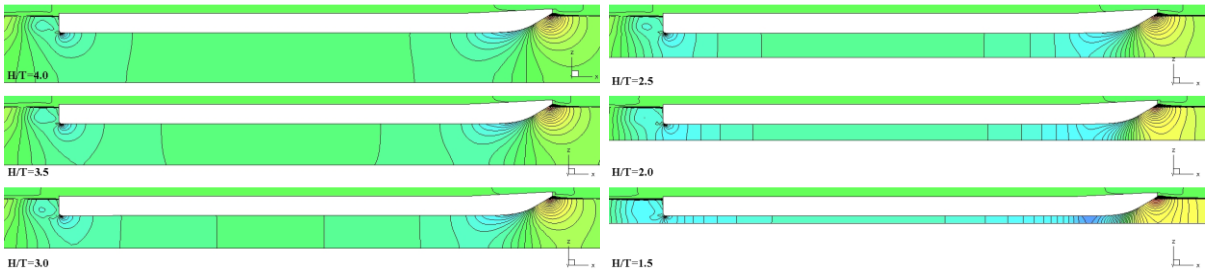

Figure 12. Pressure distribution at the ship centre line plane reference.

4. Conclusions

1. Free-surface flow around the barge hull was successfully computed. The ship's resistance, sinkage and trim were estimated by RANS-VOF CFD simulation.
2. The influence of shallow water on barge wave pattern and pressure distribution on waterway floor was successfully captured.
3. As it was expected, the most significant ship resistance change was found at H/T=1.5, v=16 km/h and v=18km/h, where the green water phenomenon was experienced. Due to the occurrence of this phenomenon we can state that the navigation on 16 and 18 km/h speeds must be avoided, proving that the ship hull shape design is not suitable for those two speeds (figures 5 and 6, tables 2 and 3).
4. For standard operation speed of 12 km/h case, the ship resistance increases from about 5% (H/T=4) to 44% (H/T=1.5), correlated to the water depth (table 3).
6. The trend of trim was inverted for the H/T=1.5 in compare to the other speeds, being experienced the highest bow trim, while for the other cases the significant aft trim was obtained (table 5).
7. The most significant sinkage has been obtained for H/T=1.5, as expected due to the highest flow velocity under the ship (table 4).

Further studies will be developed for other inland ship hull forms, in order to extend the current guidelines used for the design of ships that are operating in restricted waterway depth.

5. References

[1] Wiegmans B and Konings R 2017 *Inland Waterway Transport*: *Challenges and prospects* (London: Routledge, Taylor and Francis Group)
[2] Raven H C 2012 A computational study of shallow-water effects on ship viscous resistance *Proceedings of the 29th Symposium on Naval Hydrodynamics Gothenburg*
[3] Van der MEIJ K 2014 Promising hydrodynamic improvements for inland vessels *Proceedings of the European Inland Waterway Navigation Conference Budapest*
[4] Lungu A and Pacuraru F 2008 Wave Resistance Minimization for Ships Running under the Restricted Water Condition *Proceedings of the Numerical Towing Tank Symposium NUTTS Brest* **08** 47-52
[5] Rotteveel E and Hekkenberg RG 2015 The Influence of Shallow Water and Hull Form Variations on Inland Ship Resistance *Proceedings of the 12th International Marine Design Conference Tokyo* 11-14
[6] Jachowski J 2008 Assessment of ship squat in shallow water using CFD *Elsevier Archives of Civil and Mechanical Engineering* 27-36
[7] Tabaczek T 2008 Computation of Flow around Inland Waterway Vessel in Shallow Water *Elsevier Archives of Civil and Mechanical Engineering Vol.VIII No.1*
[8] Tezdogan T, Incecik A and Turan O 2016 Full-scale unsteady RANS simulations of vertical ship motions in shallow water *Elsevier Journal of Ocean Engineering* 131-145
[9] Deng GB, Queutey P and Visonneau M 2010 RANS Prediction of the KVLCC2 Tanker in Head Waves *9th International Conference on Hydrodynamics Shanghai*
[10] Duvigneau R,Visonneau M and Deng G.B 2003 On the role played by turbulence closures in hull shape optimization at model and full scale *J. Marine Science and Technology* **8(1)** 1–25
[11] Queutey P and Visonneau M 2007 An interface capturing method for free-surface hydrodynamic flows *Computers & Fluids* **36(9)** 1481–1510